Available online at www.sciencedirect.com
SCIENCE DIRECT®
Journal of Organometallic Chemistry 663 (2002) 108–117
Journal of Organometallic Chemistry
www.elsevier.com/locate/jorganchem

Structural and dynamic studies in solution of anionic dinuclear azolato-bridged palladium(II) complexes

Raquel de la Cruz, Pablo Espinet *, Ana M. Gallego, Jose M. Martín-Alvarez, Jesús M. Martínez-Ilarduya

Departamento de Química Inorgánica, Facultad de Ciencias, Universidad de Valladolid, E-47005 Valladolid, Spain

Received 23 May 2002; accepted 23 July 2002

Dedicated to our former mentor and always friend Pascual Royo, who pentafluorophenylated our lives

Abstract

Detailed analysis of the ^{19}F-NMR spectra of the boat-shaped complexes $(NBu_4)_2[Pd_2(\mu\text{-}LL)_2R_4]$ (R = 3,5-$C_6Cl_2F_3$) (LL = pyrazolate (pz), **1**; dimethylpyrazolate (dmpz), **2**), **HH-** (head-to-head) and **HT-** (head-to-tail) $(NBu_4)_2[Pd_2(\mu\text{-}LL)_2R_4]$ (LL = 3-methylpyrazolate (mpz), **3**; indazolate (indz), **4**), $(NBu_4)_2[Pd_2(\mu\text{-dmpz})(\mu\text{-}LL)R_4]$ (LL = mpz, **6**; indz, **7**), and $(NBu_4)_2[R_2Pd(\mu\text{-}LL)_2Pd(C_6F_5)_2]$ (LL = pz, **8**; dmpz, **9**) affords valuable structural information in solution. The substituents of the azolate ligands, which reduce the dihedral angle between the coordination planes of the two metals, place the *endo* F_{ortho} of different PdR_2 fragments at short distances. A single-crystal X-ray structure has been obtained for compound **HT-4** and the distances between F_{ortho} compared with that calculated from the NMR spectra. The study of the dynamic processes for these complexes reveals the involvement of different mechanisms such as: (a) rotation of the R groups, (b) boat–boat inversion of the six-membered Pd(μ-LL)$_2$Pd ring, (c) σ-1,2-metallotropic shift, and (d) associative exchange of PdR_2 fragments between **1** and mononuclear complexes.

Keywords: Palladium; Pyrazol; Indazol; Fluxionality; Through-space coupling

1. Introduction

Dinuclear complexes in which the metal centers are disposed near to each other by bridging ligands have attracted considerable attention. This is mainly associated to the expectation that the cooperative effects between the two metal units may have a profound influence on the reactivity and other properties of these complexes. Among the ligands capable of forming these complexes, azolates have been used extensively [1], and consequently a large amount of structural information is available. The main structural feature for dinuclear bis(azolato)complexes is the boat-like conformation of the 'M(N–N)$_2$M' six-membered metallacycle [2], which has a remarkable flexibility allowing a wide range of intermetallic distances. Surprisingly, reports describing dynamic behaviors in solution for such complexes are very scarce [3].

We have reported recently a reinvestigation of the solution behavior of $(NBu_4)_2[M_2(\mu\text{-}LL)_2R_4]$ (M = Ni, Pd, Pt; LL = pyrazolate (pz), dimethylpyrazolate (dmpz), 3-methylpyrazolate (mpz), indazolate (indz); R = C_6F_5, 2,4,6-$C_6F_3H_2$) [4], but the complete study of these systems was not carried out due to the complexity of their ^{19}F-NMR spectra. In order to get a deeper insight into the solution behavior and structures we decided to investigate the related 3,5-dichlorotrifluorophenyl (R from now) palladium complexes [5]. These give rise to more simple ^{19}F-NMR spectra due to the simpler spin system of ^{19}F nuclei within the R group and to the fact that the couplings between these nuclei (in *meta* positions) are usually less than the half-height band-width. Thus, through-space inter-ring F–F couplings can be easily observed [6], and computer simulations to obtain activation parameters for different processes can be carried out. We have reported recently

* Corresponding author. Tel.: +34-983-42-3231; fax: +34-983-42-3013
E-mail address: espinet@qi.uva.es (P. Espinet).

0022-328X/02/$ - see front matter
PII: S0022-328X(02)01772-2

the typical patterns for static ^{19}F-NMR spectra in the F_{ortho} region for *cis*-PdR_2 fragments in square-planar complexes with different symmetry elements giving rise to different chemical or magnetic equivalence situations, and the influence of several dynamic processes in these F_{ortho} signals [7].

The compounds described in this paper allow us to carry out a structural study of anionic dinuclear azolato-bridged palladium(II) complexes in solution using F–F inter-ring couplings. These are sensitive to the distortions produced by the presence of substituents in the azolate ligands. In addition, the dynamic behavior of these complexes has been investigated, revealing the occurrence of the following processes: (a) exchange of *endo* and *exo* F_{ortho}, (b) exchange of **HT** and **HH** isomers, and (c) exchange of PdR_2 fragments, for which different mechanisms have been proposed.

2. Results and discussion

2.1. Synthesis of the complexes

The complexes $(NBu_4)_2[Pd_2(\mu\text{-LL})_2R_4]$ (LL = pz, **1**; dmpz, **2**; mpz, **3**; indz, **4**) were obtained by reaction of $[PdR_2(COD)]$ with a methanol solution of H(LL) and NBu_4OH in 1:1:1 ratio (**1**, **3**, **4**), or by treatment of a solution of *cis*-$[PdR_2(Hdmpz)_2]$ in acetone with NBu_4OH in 1:1 ratio (**2**) [8]. Mixtures of **2** and $(NBu_4)_2[Pd_2(\mu\text{-dmpz})(\mu\text{-OH})R_4]$ (**5**) were obtained when the first method was used for Hdmpz. However, the reaction of $[PdR_2(COD)]$ with a methanol solution of Hdmpz and NBu_4OH in 2:1:2 ratio afforded only **5**. Treatment of **5** with H(LL) (LL = mpz, indz) in acetone produced the mixed complexes $(NBu_4)_2[Pd_2(\mu\text{-dmpz})(\mu\text{-LL})R_4]$ (**6**, **7**).

In addition, $(NBu_4)_2[R_2Pd(\mu\text{-LL})_2Pd(C_6F_5)_2]$ (LL = pz, **8**; dmpz, **9**) were detected by ^{19}F-NMR in the mixture of products resulting from the reaction of *cis*-$[Pd(C_6F_5)_2(THF)_2]$ or $[Pd(C_6F_5)_2(COD)]$ and $(NBu_4)_2[Pd_2(\mu\text{-LL})_2R_4]$ in $(CD_3)_2CO$ at room temperature, showing that these reorganization reactions proceed very fast. However, the same products **8**–**9** were detected from mixtures of $(NBu_4)_2[Pd_2(\mu\text{-LL})_2R_4]$ and $(NBu_4)_2[Pd_2(\mu\text{-LL})_2(C_6F_5)_4]$ only after heating in $(CD_3)_2CO$ at 323 K for several days.

2.2. Characterization of the complexes

Complexes **1**–**7** are white, air-stable, and were characterized by elemental analysis, spectroscopic methods, and measurements of the molar conductivity in acetone solution. Their room temperature ^{1}H-NMR spectra in $(CD_3)_2CO$ showed the characteristic resonances due to the hydrogens of the bridging azolate groups and indicated that the two diastereoisomers arising from relative head-to-head (**HH**) and head-to-tail (**HT**) disposition of the bridging ligands were present for the complexes with two unsymmetrical substituted azolates (**3**, **4**). The molar ratio between the major and the minor isomer is close to 10:1 reflecting the similar behavior of mpz and indz ligands.

Single crystals of the **HT** complex $(NBu_4)_2[Pd_2(\mu\text{-indz})_2R_4]$ (**HT-4**) were obtained by layering a dichloromethane solution with hexane. An X-ray diffraction analysis of one of them showed the boat conformation of the central Pd_2N_4 ring (vide infra). The solutions prepared at 203 K from crystalline samples obtained as described above exhibit only the major isomer (**HT-4**) while the minor isomer (**HH-4**) is formed by isomerization, slowly on standing at low temperature, or rapidly on raising the temperature, until the equilibrium is reached. These results are in accord with our previous assignation of isomers made for the analogous complexes with C_6F_5 and $C_6F_3H_2$ [4].

The room temperature ^{19}F-NMR spectra of **1**–**7** in $(CD_3)_2CO$ exhibit almost in all cases one or several broad bands in the F_{ortho} region, suggesting the occurrence of fluxional processes. Their variable temperature ^{19}F-NMR spectra have been recorded in the range 180–328 K and provide a better understanding of the dynamic behavior of dinuclear pyrazolato compounds, as we discuss below.

2.2.1. Crystal structure of the *HT* complex $(NBu_4)_2[Pd_2(\mu\text{-indz})_2R_4]$ (*HT-4*)

The structure of the $[Pd_2(\mu\text{-indz})_2R_4]^{2-}$ anion is depicted in Fig. 1. Selected atom distances and bond angles are collected in Table 1. The anion has two fold symmetry and is comprised of two Pd atoms bridged by two indazolate ligands, with a Pd(1)···Pd(1)# separation of 3.538(10) Å indicative of no metal–metal bond interaction. The two remaining coordination sites around each Pd atom are occupied by two R ligands.

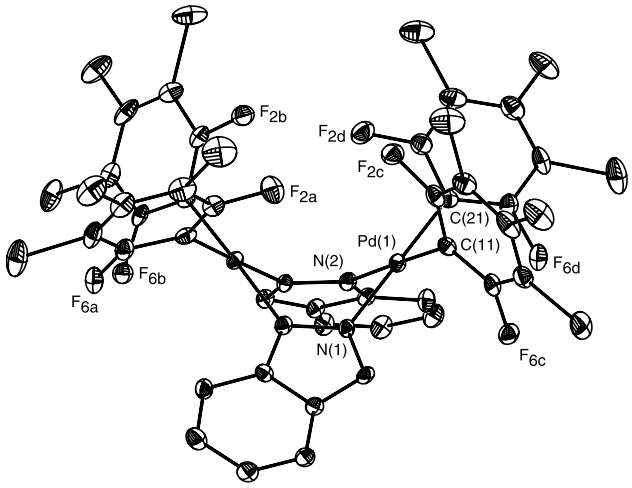

Fig. 1. ORTEP view of the anion of **HT-4** (30% probability ellipsoids).

Table 1
Selected interatomic distances (Å) and bond angles (°) for **HT-4** [a]

Bond lengths	
Pd(1)–C(11)	1.998(9)
Pd(1)–C(21)	2.005(10)
Pd(1)–N(1)	2.073(7)
Pd(1)–N(2)	2.080(7)
N(1)–N(2)#1	1.374(9)
Non-bonded distances	
F2a–F2b	3.260(12)
F2a–F2c	2.770(13)
F2a–F2d	4.308(14)
F2b–F2c	4.070(14)
F6a–F6b	2.959(12)
Pd(1)–Pd(1)#1	3.538(10)
Bond angles	
C(11)–Pd(1)–C(21)	88.1(4)
C(11)–Pd(1)–N(1)	90.3(3)
C(21)–Pd(1)–N(2)	91.6(3)
N(1)–Pd(1)–N(2)	90.0(3)
N(2)#1–N(1)–Pd(1)	120.6(6)
N(1)#1–N(2)–Pd(1)	122.1(6)

[a] Symmetry transformations used to generate equivalent atoms: #1 $-x+3/2$, $y+0$, $-z+0$.

Deviation from the least-squares plane defined by the Pd atom and the donor atoms, are 0.0071, 0.0184, −0.0146, −0.0140, and 0.0173 Å for Pd(1), C(11), C(21), N(1) and N(2) atoms, respectively. The R rings present C–C–C angles at the C_{ipso} lower than 120° (114.9(9) and 113.8(10)), as usually observed for perhalogenated aryl rings [9].

The 'Pd_2N_4' ring adopts the typical boat conformation placing the *endo* F_{ortho} of the PdR_2 moieties at very short distances. Consequently large through-space coupling constants between these nuclei are expected [10]. In addition, a tilt of two R aryl rings occurs to minimize repulsions between R and the aryl ring of the indazolate. This causes an approach of the *exo* F_{ortho} (F^6) in each PdR_2 moiety.

2.2.2. Static ^{19}F-NMR spectra of the complexes

The complexes with symmetric azolates, **1** and **2**, display in their ^{19}F-NMR spectra at 180 K two signals in the F_{ortho} region and only one signal in the F_{para} region. This is consistent with the static ^{19}F-NMR spectrum expected for a di-μ-azolate complex with a boat conformation and C_{2v} symmetry (Fig. 2), which contains four equivalent R groups and two different types of F_{ortho} (*endo* or F^2 and *exo* or F^6). These F_{ortho} signals are singlets with ca. 4 Hz band-width at half-height [7], and are clearly more deshielded (>5 ppm) for **2** than for **1**. Unfortunately, the analysis of the influence of the methyl substituents of the azolate ligands cannot be made in these complexes because the F–F through-space coupling constants have no reflect in the observed spectrum of these highly symmetric complexes. To this end, we considered the mixed

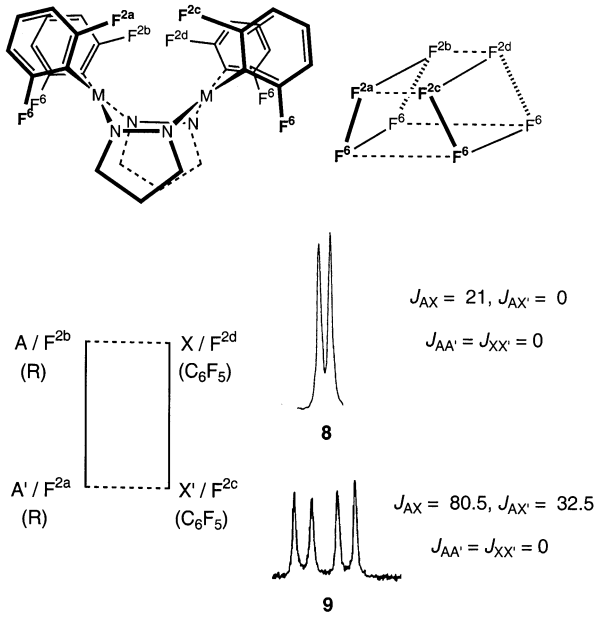

Fig. 2. Downfield F_{ortho} (R group) signals of $(NBu_4)_2[R_2Pd(\mu\text{-}LL)_2Pd(C_6F_5)_2]$ (LL = pz (**8**), dmpz (**9**)) ($(CD_3)_2CO$, 282.35 MHz, 180 K) and estimated *J* values in Hz.

complexes **8** and **9**, in which the *endo* F_{ortho} nuclei are not equivalent.

The F_{ortho} region (R group) at 180 K of **8** and **9** in $(CD_3)_2CO$ shows two signals, one singlet (upfield, F^6) and one multiplet (downfield, F^2). The appearance of the F^2 signals of R (Fig. 2) is due to the presence of inter-aryl F–F couplings with the *endo* F_{ortho} nuclei belonging to the $Pd(C_6F_5)_2$ fragments. Compared with **8**, the spectrum of **9** reflects the steric effect of the methyl substituents of the dmpz ligands. These force a reduction of the dihedral angle between the coordination planes of the two metals, bringing closer the *endo* F_{ortho} atoms on rings at different sides of the azolato bridge (2a–2c, 2b–2d, 2b–2c, 2a–2d). Consequently the coupling constants between them increase noticeably [11].

Complex **5** displays in its ^{19}F-NMR spectra (in the range 180–328 K) two signals in the F_{ortho} region and two signals in the F_{para} region. This agrees with the presence of a symmetry plane in the anion that relates the two PdR_2 fragments, and the existence of a low activation process. This could be a fast envelope-shift movement of the Pd_2N_2O ring (which is not planar; see the structure of $(NBu_4)_2[Pt_2(\mu\text{-}OH)(\mu\text{-}dmpz)(C_6F_5)_4]$) [12], or a fast fluoroaryl rotation of all the R groups around the Pd–C bond. The latter possibility is less likely considering the steric hindrance in the coordination environment of the Pd center [13].

The complexes with two asymmetric azolates, **3** and **4**, have a lower symmetry (C_2 for the **HT** isomer; C_s for the **HH** isomer). Four F_{ortho} and two F_{para} signals are expected and observed for each isomer in the slow

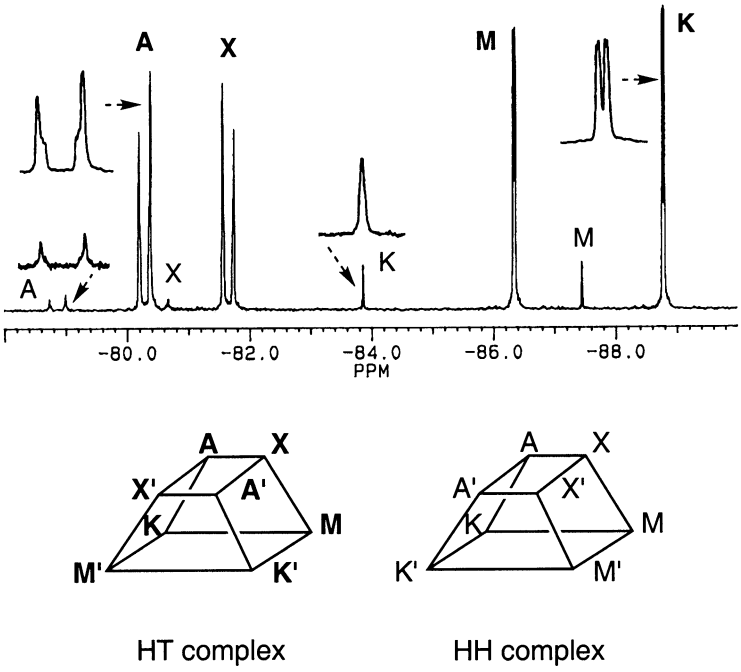

Fig. 3. F_{ortho} region of the ^{19}F-NMR spectrum of **4** ($(CD_3)_2CO$, 282.35 MHz, 248 K) and assignment of the different signals.

exchange limit (Fig. 3). The assignment of the F_{ortho} signals of each R group (A and K or X and M) is made easily using $^{19}F-^{19}F$ EXSY (EXchange SpectroscopY) experiments at higher temperatures, as we discuss later.

However, only the two upfield signals for both isomers (*exo* F_{ortho}) show the expected doublet of doublets for the **HT** complex or the expected singlet for the **HH** complex [7]. The downfield signals for both isomers (*endo* F_{ortho}) appear as somewhat distorted 'doublets' with a large coupling constant ($J_{AX}+J_{AX'} >$ 50 Hz). This is due to the non-zero through-space coupling constant J_{AX} (the scalar contribution for a $^9J_{AX}$ can be neglected). This coupling makes separate treatment of the individual PdR_2 fragments impossible, and a spin system with eight nuclei must be considered to simulate the downfield F_{ortho} signals of each isomer. The different J values estimated by simulation of the static spectra for the **HT-4** isomer (for **HT-3** the results are very similar) are collected in Table 2. These J_{F-F} values are roughly consistent with the F–F distances obtained by X-ray diffraction and confirm that, average, the tilt of the aryl groups is maintained in solution. However, the measured J_{FF} values differ noticeably from the results predicted using the Ernst's formula and the solid-state distances (Table 3). Probably the solid state packing forces distort the solution structure and a better correlation should not be expected.

The simulation of the static spectra for the **HH** isomers is more difficult and less informative, as these are minor isomers with some overlapped signals, and the magnitude of some coupling constants does not affect significantly the appearance of the spectrum. Only the large values of $J(2a–2c) = J(2b–2d) = 75$ Hz, which are bigger than in the **HT** isomers, need to be discussed. In

Table 2
$^{19}F-^{19}F$ couplings (in Hz) in selected dinuclear azolato-bridged palladium complexes [a]

	Complex/T (K)		
F–F	**HT-4**/248 [b]	**HT-6**/195 [c]	**HT-7**/195 [c]
2a–2b	5.4	0.0	0.0
2a–2c	48.0	105.0	112.6
2a–2d	0.0	0.0	0.0
2b–2c	2.5	16.3	13.0
2b–2d	48.0	59.5	62.6
2c–2d	5.4	5.0	5.8
6a–6b	8.8	9.7	10.6
6c–6d	8.8	35.5	37.6

[a] In $(CD_3)_2CO$.
[b] Pyrazolate substituents are located near positions a and d.
[c] Pyrazolate substituents are located near positions a, c and d.

Table 3
Application of the Ernst's formula to X-ray and solution data for **HT-4**

	X-ray data		Solution data	
	Distances (Å)	J (Hz) [a]	J (Hz)	Distances (Å) [a]
F2a–F2b	3.260(12)	7.8	5.4	3.375
F2a–F2c	2.770(13)	37.7	48.0	2.695
F6a–F6b	2.959(12)	20.6	8.8	3.223

[a] Calculated by the Ernst's formula.

the **HH** isomers both azolate substituents are situated close to one of the Pd atoms altering the usual shape of the boat Pd(μ-NN)$_2$Pd ring by reduction of the dihedral angle α (Fig. 4) between the coordination plane of the mentioned Pd atom and the least-square plane formed by the four N atoms of the azolate rings. This distortion produces an approach of the *endo* F_{ortho} giving a more crowded situation in the **HH** than in the **HT** isomer. This suggests that the **HH** isomer should be less stable, which is in accord with the isomer ratio found by NMR (**HT**:**HH** = 10:1).

The static spectra of the complexes **6** and **7**, which have the lowest symmetry with all the fluorine atoms chemically inequivalent, can be easily interpreted considering the spatial distribution of the azolate substituents (near positions a, c, and d), the information provided by $^{19}F-^{19}F$ EXSY experiments, and the distortions produced by the substituents of the azolate ligands by their interaction with R groups close to them. For instance, the F_{ortho} region of $(NBu_4)_2$[Pd$_2$(μ-dmpz)(μ-indz)R$_4$] (**7**) in $(CD_3)_2CO$ at 195 K (Fig. 6) can be fully assigned taking into account that J(2a–2c) should be the largest coupling constant between *endo* F_{ortho}, and that J(6c–6d) the largest between *exo* F_{ortho}.

2.3. Dynamic behavior of the complexes

We will analyze three different processes: (a) exchange of *endo* and *exo* F_{ortho}, (b) exchange of **HT** and **HH** isomers, and (c) exchange of PdR$_2$ fragments. The exchange rates were measured by magnetization transfer experiments (MT) [14], and/or line-shape analysis (LSA) [15], and the activation-energy parameters were calculated (Table 4).

The F_{ortho} signals observed at low temperature for all the di-μ-azolato complexes in $(CD_3)_2CO$ broadened soon (Figs. 5 and 6) on heating, due to the exchange of the F_{ortho} atoms of the same R rings. Other exchanges (between different R groups of the same isomer or between R groups of different isomers), which can be detected in the F_{para} region, are much slower.

The broadening of the F_{ortho} signals in complexes with inequivalent R groups indicates the existence of different activation energies for the exchange of *endo* and *exo* F_{ortho} in each R group. Surprisingly the lower energies correspond to the R groups close to the substituents of the azolate rings. This is particularly clear in **HH-3**, **HH-4** (the R groups with their F_{ortho} signals clearly more deshielded show the faster exchange) and also in **6** and **7** (Fig. 6). Additional experiments in $CDCl_3$ show similar o slightly higher activation energies for the exchange of *endo* and *exo* F_{ortho} except in the case of **1** which shows a clearly smaller value (Table 4).

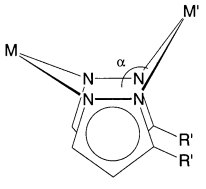

Fig. 4. Distortion of the M(μ-NN)$_2$M′ ring when the two pyrazolate substituents R′ are close to M′.

We can rule out the breaking of the Pd$_2$N$_4$ cycle, that would be energetically more demanding, should produce exchange of *endo* and *exo* F_{ortho} with the same barrier for the inequivalent R groups, and should be easier in more donor solvents such as $(CD_3)_2CO$. Among the rest of the mechanisms, we consider the following as more likely: (a) the inversion of the boat conformation of the six-membered Pd(μ-LL)$_2$Pd ring; and (b) the fluoroaryl rotation around the Pd–C bond. Theoretical calculations show that the planar non-polar conformation of the six-membered M(μ-LL)$_2$M ring seems to be accessible energetically only for LL = pz [3b]. This leaves rotation as the mechanism giving rise to F_{ortho} exchange for **2**–**4** and **6**–**7**. The change in the appearance of the F^{6d} in **7** from doublet (coupled to F^{6c}, 195 K, Fig. 6) to triplet (coupled to F^{2c} and F^{6c}, 250 K) is a proof of the rotation of R^c.

For **1**, the exchange of F_{ortho} is slower in $(CD_3)_2CO$ than in $CDCl_3$. This can be understood for a boat–boat inversion mechanism, because in that case the planar transition state is non-polar, whereas the boat-shaped ground stated is polar. Moreover, the activation parameters change dramatically with the solvent, and $\Delta S^{\ddagger}$ inverts its sign. Assuming that $\Delta S^{\ddagger}$ is importantly influenced by solvent effects, the similar behavior of **1** and **2** in $(CD_3)_2CO$ suggests that the fast process producing equivalence of the F_{ortho} for **1** in $(CD_3)_2CO$ is aryl rotation. The inversion in $\Delta S^{\ddagger}$ sign (to positive) suggests that the mechanism detected in $CDCl_3$ is different and consistent with a boat inversion. In effect, a polar non planar ground state should induce higher solvent ordering than a non polar planar transition state, giving rise to a positive $\Delta S^{\ddagger}$ value. In the more polar $(CD_3)_2CO$, the barrier for boat–boat inversion is higher than that for R rotations, and R rotation is preferred. In the less polar $CDCl_3$, the barrier for boat–boat inversion is lower, and this mechanism is faster than R rotation. The boat–boat inversion, has been previously suggested [3a–d].

Looking at the F_{para} region, $^{19}F-^{19}F$ EXSY experiments above room temperature revealed exchanges between different R groups ($R^a \leftrightarrow R^c$ and $R^b \leftrightarrow R^d$) of the same complex (**HT-3**, **HT-4**, **6** and **7**) and between R groups of different isomers (**3**, **4**). MT experiments in the F_{para} region carried out a 298 K for **6** and **7** in $CDCl_3$ showed that the free activation energy values found for this exchange are smaller for **6** (μ-dmpz-μ-mpz) than for **7** (μ-dmpz-μ-indz). The mechanism proposed to explain this kind of exchange is the so-called sliding mechanism

Table 4
Activation parameters for the different processes observed for complexes **1**, **2**, **6** and **7** (S.D. in parentheses)

Complex/solvent	Process	Method	$\Delta G^{\ddagger}_{298}$ (kJ mol^{-1})	$\Delta H^{\ddagger}$ (kJ mol^{-1})	$\Delta S^{\ddagger}$ (J K^{-1} mol^{-1})
1/$(CD_3)_2CO$	Exchange of F_{ortho}	TM + LSA	48.2(0.3)	45.09(0.18)	−10.6(0.8)
1/$CDCl_3$	Exchange of F_{ortho}	TM + LSA	38.7(1.1)	48.8(0.7)	33(3)
2/$(CD_3)_2CO$	Exchange of F_{ortho}	TM + LSA	43.4(0.8)	38.5(0.4)	−16(2)
2/$CDCl_3$	Exchange of F_{ortho}	$T_{coalescence}$	45.1(0.3) [a]		
6/$CDCl_3$	Exchange $R^b \leftrightarrow R^d$	TM	71.41(0.05)		
7/$CDCl_3$	Exchange $R^b \leftrightarrow R^d$	TM	74.95(0.04)		
1 + $[PdR_2(THF)_2]$/$(CD_3)_2CO$ [b]	Exchange of PdR_2 fragment	TM	77.62(0.08)		

[a] Calculated at 254 K due to the unstability of **2** in $CDCl_3$.
[b] [**1**] = 0.008 M.

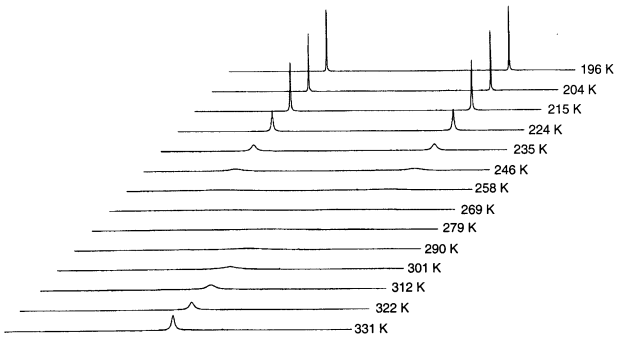

Fig. 5. Variable temperature ^{19}F-NMR spectra ($(CD_3)_2CO$, 282.35 MHz, F_{ortho} region) of $(NBu_4)_2[Pd_2(\mu\text{-pz})_2R_4]$ (**1**).

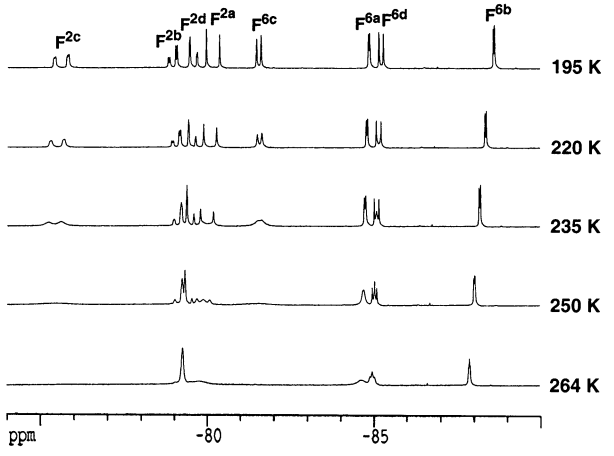

Fig. 6. Variable temperature ^{19}F-NMR spectra ($(CD_3)_2CO$, 282.35 MHz, F_{ortho} region) of $(NBu_4)_2[Pd_2(\mu\text{-dmpz})(\mu\text{-indz})R_4]$ (**7**).

[3b], which requires the breaking of at least one Pd–N bond and the exchange of the nitrogen of the monodentate azolate directly bonded to the palladium (σ-1,2-metallotropic shift) [16] before the Pd–N bond is reformed.

In addition, ^{19}F–^{19}F EXSY experiments above room temperature of 2:1 mixtures of *cis*-$[PdR_2(THF)_2]$ and $(NBu_4)_2[Pd_2(\mu\text{-pz})_2R_4]$ (**1**) in $(CD_3)_2CO$ also revealed exchanges between R groups of different PdR_2 fragments. For this process, $\Delta G^{\ddagger}_{298}$ has been obtained using MT experiments in the F_{para} region and its value suggests that probably monobridged dinuclear species, arising from dissociation of one Pd–N bond, are involved. The uncoordinated N end can then produce a nucleophilic associative substitution of ligand on the *cis*-$[PdR_2(THF)_2]$ complex. The use of less labile ligands coordinated to the PdR_2 fragment, (COD instead of THF) [17], slowed down the process to the point that it cannot be detected by MT or EXSY experiments. However, using 2:1 mixtures of $[Pd(C_6F_5)_2(COD)]$ and **1** we can detect three new species: $[PdR_2(COD)]$, $(NBu_4)_2[R_2Pd(\mu\text{-pz})_2Pd(C_6F_5)_2]$ (**8**), and $(NBu_4)_2[Pd_2(\mu\text{-LL})_2(C_6F_5)_4]$, which reach their equilibrium concentrations after a few minutes. The associative attack to a less electrophilic anionic system should be much more difficult. In fact, mixtures of **1** and $(NBu_4)_2[Pd_2(\mu\text{-pz})_2(C_6F_5)_4]$ gave **8** (molar fraction = 0.5) only after heating in $(CD_3)_2CO$ at 323 K for several days. This supports the mechanism proposed.

3. Experimental

3.1. General

Reagents and solvents used were of commercially available reagent quality. $[PdR_2(COD)]$ was prepared as previously reported [5a]. Elemental analysis for carbon, hydrogen and nitrogen was performed on a Perkin–Elmer 2400 CHN elemental analyzer. Conductivity measurements were done with a Mettler Toledo MC226 conductivimeter. Infrared spectra were recorded with a Perkin–Elmer FTIR 1720 X spectrophotometer with samples prepared as Nujol mulls. The ^{1}H- and ^{19}F-NMR measurements were performed with a Bruker ARX-300 and a Bruker AC-300 equipped with a control temperature unit VT-100. Chemical shifts (ppm) were referred to $SiMe_4$ (^{1}H) and CCl_3F (^{19}F). All the ^{1}H-NMR spectra (300.13 MHz, $(CD_3)_2CO$, 293 K) of the complexes **1**–**7** contain the characteristic resonances due to the hydrogens of the NBu_4^+ group at $\delta = 0.95$ (t, 24H, CH_3), 1.40 (m, 16H, CH_2CH_3), 1.80 (m, 16H,

NCH_2CH_2) and 3.40 (m, 16H, NCH_2). The EXSY experiments were carried out with a standard NOSEY program operating in phase sensitive mode, with a 5% of random variation of the evolution time to avoid COSY cross-peaks, with a mixing time of 0.6 s. X-ray crystallographic structure of **HT-4** was resolved in a Bruker SMART CCD diffractometer.

3.2. Synthesis

3.2.1. $(NBu_4)_2[Pd_2(\mu\text{-}LL)_2R_4]$ (LL = pz, **1**; mpz, **3**; indz, **4**)

A 40% aqueous solution of NBu_4OH (262 μl, 0.400 mmol) was added to a methanol (15 ml) solution of H(LL) (0.400 mmol). After 5 min of constant stirring the complex [PdR_2(COD)] (246 mg, 0.400 mmol) was added and the resulted solution was stirred for 8 h. For **1** and **4**, a suspension was obtained and the white solid was filtered off, washed with methanol (5 ml) and dried off. For **3**, a solution was obtained and was concentrated until 2 ml. The addition of isopropanol (5 ml) afforded **3** as a white solid that was filtered off, washed with isopropanol (5 ml) and vacuum-dried. Compound **1**: yield: 85%. $C_{62}H_{78}F_{12}Cl_8N_6Pd_2$ (1631.758): Calc.: C, 45.64; H, 4.82; N, 5.15. Found: C, 45.59; H, 4.86; N, 5.13%. IR (Nujol mulls, cm^{-1}): 1047, 771, 695, 684. ^{1}H-NMR (300.13 MHz, $(CD_3)_2CO$, 293 K) $\delta = 5.68$ (t, $J =$ 1.9 Hz, 2H, H^4), 7.03 (d, $J_{H3,H4} = J_{H4,H5} = 1.9$ Hz, 4H, $H^3 + H^5$). ^{19}F-NMR (282.35 MHz, $(CD_3)_2CO$, 220 K) $\delta = -82.13$ (s, 4F, F^2), -87.85 (s, 4F, F^6), -123.25 (s, 4F, F^4). Λ_M ($(CH_3)_2CO$, 5.0×10^{-4} M, 298.15 K) = 203.0 S cm^2 mol^{-1}. Compound **3**: yield: 75%. $C_{64}H_{82}F_{12}Cl_8N_6Pd_2$ (1659.812): Calc.: C, 46.31; H, 4.98; N, 5.06. Found: C, 46.28; H, 4.77; N, 4.90%. IR (Nujol mulls, cm^{-1}): 1046, 771, 697, 690, 682. ^{1}H-NMR (300.13 MHz, $(CD_3)_2CO$, 293 K) $\delta =$ **HT** 1.88 (s, 6H, Me^3), 5.45 (d, $J = 1.8$ Hz, 2H, H^4), 7.34 (d, $J_{H4,H5} = 1.8$ Hz, 2H, H^5); **HH** 2.16 (s, 6H, Me^3), 5.42 (d, $J = 1.8$ Hz, 2H, H^4), 6.96 (d, $J_{H4,H5} = 1.8$ Hz, 2H, H^5). Ratio **HT**/**HH** = 10:1. ^{19}F-NMR (282.35 MHz, $(CD_3)_2CO$, 220 K) $\delta =$ **HT** -80.12 (m, $N = 51.5$ Hz, 2F, F^2), -81.42 (m, $N = 51.5$ Hz, 2F, F^2), -86.00 (d, $J_{F,F} = 6.0$ Hz, 2F, F^6), -88.46 (d, $J_{F,F} = 6.0$ Hz, 2F, F^6), -123.92 (s, 2F, F^4), -124.24 (s, 2F, F^4); **HH** -77.88 (m, $N = 74.8$ Hz, 2F, F^2), -80.20 (partially overlapped, F^2), -83.72 (s, 2F, F^6), -86.88 (s, 2F, F^6), -123.74 (s, 2F, F^4), -123.80 (s, 2F, F^4). Λ_M ($(CH_3)_2CO$, 5.0×10^{-4} M, 298.15 K) = 182.2 S cm^2 mol^{-1}. Compound **4**: yield: 85%. $C_{70}H_{82}F_{12}Cl_8N_6Pd_2$ (1731.879): Calc.: C, 48.55; H, 4.77; N, 4.85. Found: C, 48.54; H, 4.60; N, 4.75%. IR (Nujol mulls, cm^{-1}): 1207, 908, 807, 759, 697, 691, 683. ^{1}H-NMR (300.13 MHz, $(CD_3)_2CO$, 293 K) $\delta =$ **HT** 6.57 (ddd, $J_{H,H} = 8.0$, 6.6, 1.0 Hz, 2H, H^5 indz), 6.75 (ddd, $J_{H,H} = 8.6$, 6.6, 1.0 Hz, 2H, H^6 indz), 7.34 (dt, $J_{H,H} =$ 8.0, 1.0 Hz, 2H, H^4 indz), 7.47 (dc, $J_{H,H} = 8.6$, 1.0 Hz, 2H, H^7 indz), 8.10 (d, $J_{H,H} = 1.0$ Hz, 2H, H^3 indz) (coupling constants in the indz ring: $J_{H6,H7} = 8.6$ Hz, $J_{H4,H5} = 8.0$ Hz, $J_{H5,H6} = 6.6$ Hz, $J_{H3,H7} = J_{H4,H6} = J_{H4,H7} = J_{H5,H7} = 1.0$ Hz); **HH** 6.60 (ddd, $J_{H,H} = 8.0$, 6.6, 1.0 Hz, 2H, H^5 indz), 6.86 (ddd, $J_{H,H} = 8.6$, 6.6, 1.0 Hz, 2H, H^6 indz), 7.30 (dt, $J_{H,H} = 8.0$, 1.0 Hz, 2H, H^4 indz), 7.75 (d, $J_{H,H} = 1.0$ Hz, 2H, H^3 indz), 7.93 (dc, $J_{H,H} = 8.6$, 1.0 Hz, 2H, H^7 indz), (coupling constants in the indz ring: $J_{H6,H7} = 8.6$ Hz, $J_{H4,H5} = 8.0$ Hz, $J_{H5,H6} =$ 6.6 Hz, $J_{H3,H7} = J_{H4,H6} = J_{H4,H7} = J_{H5,H7} = 1.0$ Hz). Ratio **HT**/**HH** = 10:1. ^{19}F-NMR (282.35 MHz, $(CD_3)_2CO$, 220 K) $\delta =$ **HT** -80.25 (m, $N = 51.6$ Hz, 2F, F^2), -81.79 (m, $N = 51.6$ Hz, 2F, F^2), -86.43 (d, $J_{F,F} = 7.1$ Hz, 2F, F^6), -88.81 (d, $J_{F,F} = 7.1$ Hz, 2F, F^6), -123.19 (s, 2F, F^4), -123.25 (s, 2F, F^4); **HH** -78.94 (m, $N = 75.8$ Hz, 2F, F^2), -80.64 (m, $N = 75.8$ Hz, 2F, F^2), -83.95 (s, 2F, F^6), -87.56 (s, 2F, F^6), -122.68 (s, 2F, F^4), -123.37 (s, 2F, F^4). Λ_M (acetone, 5.0×10^{-4} M, 298.15 K) = 174.0 S cm^2 mol^{-1}.

3.2.2. cis-$[PdR_2(Hdmpz)_2]$

Hdmpz (54.8 mg, 0.570 mmol) was added to a solution of [PdR_2(COD)] (350 mg, 0.570 mmol) in chloroform (60 ml). After 30 min of stirring, the solution was evaporated to dryness and the residue was triturated with hexane (20 ml), filtered off, washed with hexane (5 ml) and vacuum-dried. Yield: 90%. $C_{22}H_{16}Cl_4F_6N_4Pd$ (698.602): Calc.: C, 37.82; H, 2.31; N, 8.02. Found: C, 37.79; H, 2.33; N, 7.96%. IR (Nujol mulls, cm^{-1}): 3436 (m, st N–H). ^{1}H-NMR (300.13 MHz, $CDCl_3$, 293 K) $\delta = 2.14$ (s, 6H, Me^3), 2.16 (s, 6H, Me^5), 5.79 (d, $J_{H1,H4} = 2.3$ Hz, 2H, H^4), 9.83 (a, 2H, H^1). ^{19}F-NMR (282.35 MHz, $CDCl_3$, 293 K) δ -91.37 (s, 4F, $F^{2,6}$), -119.79 (s, 2F, F^4).

3.2.3. $(NBu_4)_2[Pd_2(\mu\text{-}dmpz)_2R_4]$ (**2**)

A 40% aqueous solution of NBu_4OH (262 μl, 0.400 mmol) was added to a solution of *cis*-[PdR_2(Hdmpz)$_2$] (279 mg, 0.399 mmol) in acetone (15 ml). After 30 min of constant stirring the solution obtained was concentrated until 2 ml and isopropanol (10 ml) was added. The white solid obtained was filtered off, washed with isopropanol (5 ml) and vacuum-dried. Yield: 75%. $C_{66}H_{86}F_{12}Cl_8N_6Pd_2$ (1687.866): Calc.: C, 46.97; H, 5.14; N, 4.98. Found: C, 46.63; H, 4.94; N, 4.88%. IR (Nujol mulls, cm^{-1}): 1530, 1048, 773, 697, 684. ^{1}H-NMR (300.13 MHz, $(CD_3)_2CO$, 293 K) $\delta = 2.12$ (s, 12H, Me^3, Me^5), 5.14 (s, 2H, H^4). ^{19}F-NMR (282.35 MHz, $(CD_3)_2CO$, 195 K) $\delta = -76.02$ (s, 4F, F^2), -82.83 (s, 4F, F^6), -124.10 (s, 4F, F^4). Λ_M ($(CH_3)_2CO$, 5.0×10^{-4} M, 298.15 K) = 168.6 S cm^2 mol^{-1}.

3.2.4. $(NBu_4)_2[Pd_2(\mu\text{-}dmpz)(\mu\text{-}OH)R_4]$ (**5**)

A 40% aqueous solution of NBu_4OH (525 μl, 0.801 mmol) was added to a solution of Hdmpz (38.5 mg, 0.400 mmol) in methanol (200 ml). After 5 min of

constant stirring, the complex [PdR_2(COD)] (492 mg, 0.801 mmol) was added and the mixture was stirred for 8 h. The solvent was then partially evaporated under vacuum until precipitation of a white solid, which was separated by filtration, washed with methanol (5 ml) and vacuum-dried. Yield: 70%. $C_{61}H_{80}Cl_8F_{12}N_4OPd_2$ (1609.749): Calc.: C, 45.52; H, 5.01; N, 3.48. Found: C, 45.30; H, 4.80; N, 3.36%. IR (Nujol mulls, cm^{-1}): 3623 (m, st O–H), 1040, 771, 696, 684. ^{1}H-NMR (300.13 MHz, $CDCl_3$, 293 K) $\delta = -1.64$ (s, 1H, OH), 1.55 (s, 6H, Me), 5.30 (s, 1H, H^4). ^{19}F-NMR (282.35 MHz, $CDCl_3$, 293 K) $\delta = -83.89$ (s, 4F, $F^{2,6}$), -84.32 (s, 4F, $F^{2,6}$), -123.08 (s, 2F, F^4), -124.28 (s, 2F, F^4). Λ_M ($(CH_3)_2CO$, 5.0×10^{-4} M, 298.15 K) = 126.7 S cm^2 mol^{-1}.

3.2.5. $(NBu_4)_2[Pd_2(\mu\text{-dmpz})(\mu\text{-LL})R_4]$ (LL = mpz, **6**; indz, **7**)

H(LL) (0.311 mmol) was added to a solution of $(NBu_4)_2$[Pd_2(μ-dmpz)(μ-OH)R_4] (500 mg, 0.31 mmol) in acetone (50 ml). After 2 h of constant stirring the solution obtained was concentrated until 2 ml and isopropanol (10 ml) was added. The white solid precipitated was filtered off, washed with isopropanol (5 ml) and vacuum-dried. Compound **6**: yield: 75%. $C_{65}H_{84}Cl_8F_{12}N_6Pd_2$ (1673.839): Calc.: C, 46.64; H, 5.06; N, 5.02. Found: C, 46.37; H, 5.09; N, 4.92%. IR (Nujol mulls, cm^{-1}): 1587, 1048, 771, 687, 679. ^{1}H-NMR (300.13 MHz, $(CD_3)_2CO$, 293 K) $\delta = 1.80$ (s, 3H, Me dmpz), 2.00 (s, 3H, Me^3 mpz), 2.30 (s, 3H, Me dmpz), 5.19 (s, 1H, H^4 dmpz), 5.39 (d, $J = 1.7$ Hz, 1H, H^4 mpz), 7.38 (d, $J_{H4,H5} = 1.7$ Hz, 1H, H^5 mpz). ^{19}F-NMR (285.35 MHz, $(CD_3)_2CO$, 195 K) $\delta = -74.88$ (ddd, $J_{F,F} = 105.0$, 16.3, 5.0 Hz, 1F, F^{2c}), -78.91 (m, A part of an ABX system, $J_{F,F} = 59.5$, 16.3 Hz, 1F, F^{2b}), -79.33 (m, B part of an ABY system, $J_{F,F} = 59.5$, 5.0 Hz, 1F, F^{2d}), -80.13 (d, $J_{F,F} = 105.0$ Hz, 1F, F^{2a}), -81.55 (d, $J_{F,F} = 35.5$ Hz, 1F, F^{6c}), -84.86 (d, $J_{F,F} = 9.7$, 1F, F^{6a}), -85.33 (d, $J_{F,F} = 35.5$ Hz, 1F, F^{6d}), -88.07 (d, $J_{F,F} = 9.7$ Hz, 1F, F^{6b}), -123.79 (s, 2F, F^4), -124.11 (s, 1F, F^4), -124.24 (s, 1F, F^4). Λ_M ($(CH_3)_2CO$, 5.0×10^{-4} M, 298.15 K) 164.8 S cm^2 mol^{-1}. Compound **7**: yield: 77%. $C_{68}H_{84}Cl_8F_{12}N_6Pd_2$ (1709.873): Calc.: C, 47.77; H, 4.95; N, 4.91. Found: C, 47.67; H, 4.90; N, 4.91%. IR (Nujol mulls, cm^{-1}): 1206, 1048, 771, 697, 680. ^{1}H-NMR (300.13 MHz, $(CD_3)_2CO$, 293 K) $\delta = 1.83$ (s, 3H, Me dmpz), 2.23 (s, 3H, Me dmpz), 5.16 (s, 1H, H^4 dmpz), 6.54 (ddd, $J_{H,H} = 8.1$, 6.6, 1.0 Hz, 1H, H^5 indz), 6.76 (ddd, $J_{H,H} = 8.5$, 6.6, 1.0 Hz, 1H, H^6 indz), 7.29 (dt, $J_{H,H} = 8.1$, 1.0 Hz, 1H, H^4 indz), 7.72 (dc, $J_{H,H} = 8.5$, 1.0 Hz, 1H, H^7 indz), 8.12 (d, $J_{H,H} = 1.0$ Hz, 1H, H^3 indz) (coupling constants in the indz ring: $J_{H6,H7} = 8.5$ Hz, $J_{H4,H5} = 8.1$ Hz, $J_{H5,H6} = 6.6$ Hz, $J_{H3,H7} = J_{H4,H6} = J_{H4,H7} = J_{H5,H7} = 1.0$ Hz). ^{19}F-NMR (282.35 MHz, $(CD_3)_2CO$, 195 K) $\delta = -75.60$ (ddd, $J_{F,F} = 112.6$, 13.0, 5.8 Hz, 1F, F^{2c}), -78.95 (m, A part of an ABX system, $J_{F,F} = 62.6$, 13.0 Hz, 1F, F^{2b}), -79.53 (m, B part of an ABY system, $J_{F,F} = 62.6$, 5.8 Hz, 1F, F^{2d}), -80.15 (d, $J_{F,F} = 112.6$ Hz, 1F, F^{2a}), -81.54 (d, $J_{F,F} = 37.6$ Hz, 1F, F^{6c}), -84.86 (d, $J_{F,F} = 10.6$, 1F, F^{6a}), -85.22 (d, $J_{F,F} = 37.6$ Hz, 1F, F^{6d}), -88.62 (d, $J_{F,F} = 10.6$ Hz, 1F, F^{6b}), -123.29 (s, 1F, F^4), -123.53 (s, 1F, F^4), -123.65 (s, 1F, F^4), -123.79 (s, 1F, F^4). Λ_M ($(CH_3)_2CO$, 5.0×10^{-4} M, 298.15 K) = 158.8 S cm^2 mol^{-1}.

3.3. X-ray crystallography

Suitable single crystals of compound **HT-4** were mounted in glass fibers, and diffraction measurements were made using a Bruker SMART CCD area-detector diffractometer with Mo–K_α radiation ($\lambda = 0.71073$ Å) [18]. Intensities were integrated from several series of exposures, each exposure covering 0.3° in ω, the total data set being a hemisphere [19]. Absorption corrections were applied, based on multiple and symmetry-equivalent measurements [20]. The crystal was poor diffracting and the reflections with 2θ higher than 41.64° were rejected. The structure was solved by direct methods and refined by least-squares on weighted F^2 values for all

Table 5
Crystal data and structure refinement for **HT-4**

Empirical formula	$C_{70}H_{82}Cl_8F_{12}N_6Pd_2$
Formula weight	1731.82
Temperature (K)	293(2)
Wavelength (Å)	0.71073
Crystal system	Orthorhombic
Space group	*Ibca*
Unit cell dimensions	
a (Å)	24.914(3)
b (Å)	25.063(3)
c (Å)	26.023(3)
α (°)	90
β (°)	90
γ (°)	90
Volume ($Å^3$)	16249(4)
Z	8
D_{calc} (Mg m^{-3})	1.416
Absorption coefficient (mm^{-1})	0.775
$F(000)$	7040
Crystal size (mm)	0.25 × 0.21 × 0.08
θ Range for data collection (°)	1.57–20.82
Index ranges	$0 \le h \le 24$, $0 \le k \le 25$, $0 \le l \le 26$
Reflections collected	29810
Independent reflections	4254 [$R_{int} = 0.0827$]
Completeness to $\theta = 20.82°$	100.0%
Absorption correction	SADABS
Max/min transmission	1.000000, 0.724544
Refinement method	Full-matrix least-squares on F^2
Data/restraints/parameters	4254/0/447
Final R indices [$I > 2\sigma(I)$]	$R_1 = 0.0521$, $wR_2 = 0.1694$
R indices (all data)	$R_1 = 0.0886$, $wR_2 = 0.1908$
Goodness-of-fit on F^2	1.061
Largest difference peak and hole (e $Å^{-3}$)	1.072 and −0.289

reflections (see Table 5) [21]. All non-hydrogen atoms were assigned anisotropic displacement parameters and refined without positional constraints. Hydrogen atoms were taken into account at calculated positions and their positional parameters were refined. Refinement proceeded smoothly to give $R_1 = 0.0521$ based on the reflections with $I > 2\sigma(I)$. Complex neutral-atom scattering factors were used [22].

4. Supplementary material

Crystallographic data (excluding structure factors) for this structure have been deposited with the Cambridge Crystallographic Data Centre as Supplementary publication no. CCDC-185911. Copies of the data can be obtained free of charge on application to The Director, CCDC, 12 Union Road, Cambridge CB2 1EZ, UK (Fax: +44-1223-336033; e-mail: deposit@ccdc.cam.ac.uk or www: http://www.ccdc.cam.ac.uk).

Acknowledgements

We are very grateful for financial support by the Dirección General de Enseñanza Superior (Project BQU2001-2015) and the Junta de Castilla y León (Project VA120/01). The Ministerio de Educación y Cultura is gratefully acknowledged for a fellowship to A.M.G.

References

[1] (a) A.P. Sadimenko, Adv. Heterocycl. Chem. 80 (2001) 157;
(b) L.A. Oro, M.A. Ciriano, C. Tejel, Pure Appl. Chem. 70 (1998) 779;
(c) G. La Monica, G.A. Ardizzoia, Prog. Inorg. Chem. 46 (1997) 151;
(d) A.P. Sadimenko, S.S. Basson, Coord. Chem. Rev. 147 (1996) 247;
(e) S. Trofimenko, Chem. Rev. 93 (1993) 943;
(f) S. Trofimenko, Prog. Inorg. Chem. 34 (1986) 115.

[2] Only a few examples of a chair conformation have been reported:
(a) J.A. Bailey, S.L. Grundy, S.R. Stobart, Organometallics 9 (1990) 536;
(b) L.A. Oro, D. Carmona, M.P. Lamata, Inorg. Chim. Acta 97 (1985) 19;
(c) B.F. Fieselmann, G.D. Stucky, Inorg. Chem. 17 (1978) 2074.

[3] References which contain activation parameters: (a) G.W. Bushnell, D.O.K. Fjeldsted, S.R. Stobart, J. Wang, Organometallics 15 (1996) 3785;
(b) C. Tejel, J.M. Villoro, M.A. Ciriano, J.A. López, E. Eguizábal, F.J. Lahoz, V.I. Bakhmutov, L.A. Oro, Organometallics 15 (1996) 2967;
(c) C. López, J.A. Jiménez, R.M. Claramunt, M. Cano, J.V. Heras, J.A. Campo, E. Pinilla, A. Monge, J. Organomet. Chem. 511 (1996) 115;
(d) C. Tejel, M.A. Ciriano, A.J. Edwards, F.J. Lahoz, L.A. Oro, Organometallics 19 (2000) 4968;
References without activation parameters: (e) C. Tejel, M.A. Ciriano, A.J. Edwards, F.J. Lahoz, L.A. Oro, Organometallics 16 (1997) 45;
(f) C. Tejel, M.A. Ciriano, J.A. López, F.J. Lahoz, L.A. Oro, Organometallics 19 (2000) 497;
(g) C. Tejel, M.A. Ciriano, L.A. Oro, A. Tiripicchio, F. Ugozzoli, Organometallics 20 (2001) 1676.

[4] P. Espinet, A.M. Gallego, J.M. Martínez-Ilarduya, E. Pastor, Inorg. Chem. 39 (2000) 975.

[5] (a) P. Espinet, J.M. Martínez-Ilarduya, C. Pérez-Briso, A.L. Casado, M.A. Alonso, J. Organomet. Chem. 551 (1998) 9;
(b) A.L. Casado, P. Espinet, Organometallics 17 (1998) 954;
(c) A.L. Casado, J.A. Casares, P. Espinet, Inorg. Chem. 37 (1998) 4154;
(d) A.L. Casado, P. Espinet, J. Am. Chem. Soc. 120 (1998) 8978;
(e) A.L. Casado, J.A. Casares, P. Espinet, Organometallics 16 (1997) 5730.

[6] Selected references about F–F through-space coupling: (a) J.E. Peralta, V. Barone, R.H. Contreras, D.G. Zaccari, J.P. Snyder, J. Am. Chem. Soc. 123 (2001) 9162;
(b) L. Ernst, K. Ibrom, K. Marat, R.H. Mitchell, G.J. Bodwell, G.W. Bushnell, Chem. Ber. 127 (1994) 1119;
(c) C.G. Giribet, M.C. Ruiz de Azúa, R.H. Contreras, R. Lobayan de Bonczok, G.A. Aucar, S.J. Gómez, Mol. Struc. 300 (1993) 467;
(d) P. Szczecinski, J. Zachara, J. Organomet. Chem. 447 (1993) 241;
(e) F.B. Mallory, C.W. Mallory, M.B. Baker, J. Am. Chem. Soc. 112 (1990) 2577;
(f) R.S. Matthews, J. Fluorine Chem. 48 (1990) 7;
(g) F.B. Mallory, C.W. Mallory, W.M. Ricker, J. Org. Chem. 50 (1985) 457.

[7] M.A. Alonso, J.A. Casares, P. Espinet, J.M. Martínez-Ilarduya, C Pérez-Briso, Eur. J. Inorg. Chem. (1998) 1745.

[8] G. López, J. Ruiz, C. Vicente, J.M. Martí, G. García, P.A. Chaloner, P.B. Hitchcock, R.M. Harrison, Organometallics 11 (1992) 4090.

[9] P.G. Jones, J. Organomet. Chem. 345 (1988) 405.

[10] L. Ernst, K. Ibrom, Angew. Chem. Int. Ed. Engl. 34 (1995) 1881.

[11] The impossibility to prepare other similar complexes such as $(NBu_4)_2[Pd(\mu\text{-dmpz})_2(C_6Cl_5)_4]$ (G. López, J. Ruiz, G. García, J.M. Martí, G. Sánchez, J. García, J. Organomet. Chem. 421 (1991) 435) and $(NBu_4)_2[Ni_2(\mu\text{-dmpz})_2(C_6F_5)_4]$ (G. López, G. García, G. Sánchez, J. García, J. Ruiz, J.A. Hermoso, A. Vegas, M. Martínez-Ripoll, Inorg. Chem. 31 (1992) 1518) is most probably due to the strong steric repulsions between the *endo* X_{ortho}.

[12] G. López, J. Ruiz, G. García, C. Vicente, V. Rodríguez, G. Sánchez, J.A. Hermoso, M. Martínez-Ripoll, J. Chem. Soc. Dalton Trans. (1992) 1681.

[13] J.A. Casares, P. Espinet, J.M. Martínez-Ilarduya, Y.-S. Lin, Organometallics 16 (1997) 770.

[14] (a) J. Sandström, Dynamic NMR Spectroscopy (Chapter 4), Academic Press, London, 1982;
(b) J.-J. Delpuech, in: J.-J. Delpuech (Ed.), Dynamics of Solutions and Fluid Mixtures by NMR (Chapter 3), Wiley, Chichester, 1995, p. 3.

[15] DNMR6, Quantum Chemical Program Exchange (QCPE 633), Indiana University, Bloomington, IN, 1995.

[16] S. Alvarez, M.J. Bermejo, J. Vinaixa, J. Am. Chem. Soc. 109 (1987) 5316.

[17] The THF ligands are readily displaced by $(CD_3)_2CO$ and H_2O. See reference [5a].

[18] SMART V5.051 diffractometer control software, Bruker Analytical X-ray Instruments Inc., Madison, WI, 1998.
[19] SAINT V6.02 integration software, Bruker Analytical X-ray Instruments Inc., Madison, WI, 1999.
[20] G.M. Sheldrick, SADABS: A Program for Absorption Correction with the Siemens SMART system, University of Göttingen, Germany, 1996.
[21] SHELXTL program system version 5.1; Bruker Analytical X-ray Instruments Inc., Madison, WI, 1998.
[22] International Tables for Crystallography, vol. C, Kluwer, Dordrecht, 1992.